Thermal entanglement in the mixed three-spin XXZ Heisenberg model on a triangular cell*

Seyit Deniz Han and Ekrem Aydiner†

Department of Physics, İstanbul University, İstanbul Tr-34134, *Turkey*

(Received 30 July 2013; revised manuscript received 18 October 2013; published online 18 March 2014)

We numerically investigate the thermal entanglements of spins (1/2, 1) and spins (1/2, 1/2) in the three-mixed (1/2, 1, 1/2) anisotropic Heisenberg XXZ spin system on a simple triangular cell under an inhomogeneous magnetic field. We show that the external magnetic field induces strong plateau formation in the pairwise thermal entanglement for fixed parameters of the Hamiltonian in the cases of ferromagnetic and antiferromagnetic interactions. We also observe an unexpected critical point at finite temperature in the thermal entanglement of spins (1/2, 1) for the antiferromagnetic case, while the entanglement of spins (1/2, 1) in the ferromagnetic case and the entanglement of spins (1/2, 1/2) in both ferromagnetic and antiferromagnetic cases almost decay exponentially to zero with increasing temperature. The critical point in the entanglement of spins (1/2, 1) in the antiferromagnetic case may be a signature of the quantum phase transition at finite temperature.

Keywords: quantum entanglement, quantum phase transition, negativity

PACS: 03.65.Ud, 64.70.Tg **DOI:** 10.1088/1674-1056/23/5/050305

1. Introduction

It is known that quantum entanglement in spin systems plays a crucial role for various applications, such as quantum information,[1] quantum computation,[2–7] quantum teleportation,[8] superdense coding,[9] quantum communication,[10–12] quantum perfect state transfer,[13] quantum cryptology,[14,15] and quantum computational speed-ups.[16,17] Potential applications of the spin–spin entanglement in these fields have stimulated research on methods to quantify and control it. Therefore, many detailed theoretical and experimental studies have been performed to understand the quantum entanglement behavior in two and more qubits which consist of spin-half, mixed-spin, or higher Heisenberg (XX, XY, XXZ, and XYZ) and Ising spin systems.

Recently, it has been shown that the molecular spin ring, the triangular spin cell, or other spin lattice configurations have an important potential in computation and information sciences as a entanglement resource. On the other hand, it is known that the entanglement in a mixed spin system with a certain geometry may produce richer behavior than a simple spin system, i.e., two or more identical spin systems. For instance, the three-qubit entangled states have been shown to possess advantages over the two-qubit states in quantum teleportation,[18,19] dense coding,[20] and quantum colonizing.[21] However, there are limited works on the mixed-spin systems with different lattice (triangular or square) configurations in the literature.[22,23] It is important to clarify the entanglement behaviors of different spin systems which consist of mixed spins with different lattice configurations. Therefore, in this paper, we focus on the entanglement of a three-spin (1/2, 1, 1/2) anisotropic Heisenberg XXZ system on a simple triangular cell under an inhomogeneous magnetic field at equilibrium. We will show that the external magnetic field induces a strong plateau formation in thermal entanglement in the ferromagnetic (F) and the antiferromagnetic (AF) XXZ models and an unexpected critical point in entanglement occurs at finite temperature for the AF interaction.

The paper is organized as follows. In Section 2, the model and the method are introduced. In Section 3, we numerically obtain the pairwise thermal entanglement between qubits in the model and we discuss the signature of quantum phase transition. Conclusions are given in Section 4.

2. Model and method

The three-spin (1/2, 1, 1/2) anisotropic Heisenberg XXZ system on a simple triangular cell is schematically illustrated in Fig. 1 with interacting couplings. Spin-1/2 and spin-1 are represented by a black circle and a white circle, respectively. As can be seen from Fig. 1, the triangular cell with spins can be mapped to a one-dimensional system. Now, the one-dimensional spin system can be considered as a qutrit-qubits system.

*Project supported by İstanbul University (Grant Nos. 19240 and 28432).

†Corresponding author. E-mail: ekrem.aydiner@istanbul.edu.tr

© 2014 Chinese Physical Society and IOP Publishing Ltd

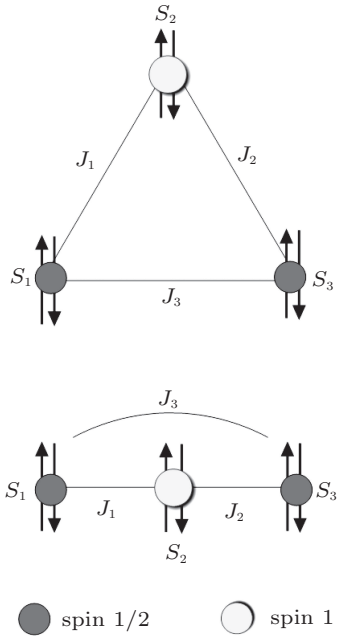


Fig. 1. Triangle lattice representation of the mixed spin system with three spins, the coupling constants are also indicated.

The Hamiltonian of the three-spin (1/2, 1, 1/2) anisotropic Heisenberg XXZ system on a one-dimensional lattice under an inhomogeneous magnetic field is given as

$$H = \sum_{i=1}^{3}[J(s_i^x s_{i+1}^x + s_i^y s_{i+1}^y) + \gamma(s_i^z s_{i+1}^z)] + (B+b)s_1^z + Bs_2^z + (B-b)s_3^z, \quad (1)$$

where $s_i^{x,y,z}$ $(i = 1,2,3)$ represent the spin operators of the spin-1/2 and spin-1 components, and the exchange interaction parameters are chosen as $J = J_1 = J_2 \neq J_3$ $(J_3 = \gamma)$. Here J denotes the exchange interaction between the nearest-neighbor spin pairs, γ is the anisotropy parameter $(-1 \leq \gamma \leq 1)$; B and b are the strengths of the homogenous and the stagger magnetic fields, respectively. The spin chain has a ferromagnetic interaction when $J < 0$ and an antiferromagnetic interaction when $J > 0$. The periodic boundary condition $s_3^{x,y} = s_1^{x,y}$ is applied.

Hamiltonian (1) can be rewritten in the matrix form as

$$H = \begin{pmatrix}
2B+5\xi & 0 & 0 & 0 & 0 & 0 & 0 & 0 & 0 & 0 & 0 & 0 \\
0 & B+\eta & \lambda & 0 & 0 & 0 & \alpha & 0 & 0 & 0 & 0 & 0 \\
0 & \lambda & B+\xi & 0 & 0 & 0 & \lambda & 0 & 0 & 0 & 0 & 0 \\
0 & 0 & 0 & b-\xi & \lambda & 0 & 0 & \lambda & \alpha & 0 & 0 & 0 \\
0 & 0 & 0 & \lambda & -3\xi & 0 & 0 & 0 & \lambda & 0 & 0 & 0 \\
0 & 0 & 0 & 0 & 0 & \eta-B & 0 & 0 & 0 & \lambda & \alpha & 0 \\
0 & \alpha & \lambda & 0 & 0 & 0 & \zeta+B & 0 & 0 & 0 & 0 & 0 \\
0 & 0 & 0 & \lambda & 0 & 0 & 0 & -3\xi & \lambda & 0 & 0 & 0 \\
0 & 0 & 0 & \alpha & \lambda & 0 & 0 & \lambda & \zeta & 0 & 0 & 0 \\
0 & 0 & 0 & 0 & 0 & \lambda & 0 & 0 & 0 & -B+\xi & \lambda & 0 \\
0 & 0 & 0 & 0 & 0 & \alpha & 0 & 0 & 0 & \lambda & \zeta-B & 0 \\
0 & 0 & 0 & 0 & 0 & 0 & 0 & 0 & 0 & 0 & 0 & -2B+5\xi
\end{pmatrix}, \quad (2)$$

where $\xi = \gamma/4$, $\lambda = J/\sqrt{2}$, $\alpha = J/2$, $\eta = b - \xi$, $\zeta = -(b+\xi)$. The basis vectors of Hamiltonian matrix (2) are $\{|-1/2,-1,-1/2\rangle$, $|1/2,-1,-1/2\rangle$, $|-1/2,-1,1/2\rangle$, $|1/2,-1,1/2\rangle$, $|-1/2,0,-1/2\rangle$, $|1/2,0,-1/2\rangle$, $|-1/2,0,1/2\rangle$, $|1/2,0,1/2\rangle$, $|-1/2,1,-1/2\rangle$, $|1/2,1,-1/2\rangle$, $|-1/2,1,1/2\rangle$, $|1/2,1,1/2\rangle\}$, where $|s_1,s_2,s_3\rangle$ is the eigenstate of s_1^z, s_2^z, s_3^z with the corresponding eigenvalues of matrix (2).

In order to obtain the thermal entanglement for Hamiltonian (1), we use the concept of the negativity. It is known that entanglement in spin-half systems can be measured by using concurrence, which is applicable to an arbitrary state of two spin-1/2.[24] For systems which consist of higher spins, the thermal entanglement of the spin system can be analyzed by using the negativity. The negativity, which is the quantitative version of the Peres–Horodecki criterion,[25,26] was proposed by Vidal and Werner.[27] They presented that the entanglement for higher spins can be computed efficiently by using the negativity, and the negativity does not increase under local manipulations of the system. The negativity is defined, depending on the density operator $\rho(T)$, by

$$N(\rho) = \sum_i |\mu_i|, \quad (3)$$

where μ_i is the negative eigenvalue of the partial transpose $\rho(T)^{t_1}$. Here t_1 and $\rho(T)$ are the partial transpose with respect to the first system and the density operator, respectively. The density operator $\rho(T) = \exp(-H/kT)/Z$ represents the state of the system at thermal equilibrium, where $Z = \mathrm{Tr}(\exp(-H/kT))$ is the partition function, H is the Hamiltonian matrix, T is the temperature, and k is Boltzmann's constant which we take to be 1 for the sake of simplicity. Equation (3) can also be written with the trace norm of ρ^{t_1} as

$$N(\rho) = \frac{\|\rho(t)^{t_1}\| - 1}{2}, \quad (4)$$

where the trace norm of ρ^{t_1} is equal to the sum of the absolute values of the eigenvalues of ρ^{t_1}.

The negativities N_{12} and N_{13} correspond to the entanglements between spins (1/2, 1) and between spins (1/2, 1/2), re-

spectively. Therefore, the entanglement in each spin pair in this model can be investigated separately. The computation of negativities N_{12} and N_{13} require the partial transposes of the reduced density matrices, which are derived from the density matrix ρ of Hamiltonian (2). To investigate the thermal entanglement of this system, we follow a simple procedure. In the first step, the Hamiltonian is written in a block-diagonal form in the Hilbert space, as shown in Eq. (2), and density matrix ρ is obtained by using the eigenvalues and the eigenstates of Hamiltonian matrix (2). In the second step, the reduced density matrices of ρ are obtained by tracing out with respect to the related spin, then the pairwise negativities (N_{12} and N_{13}) are computed according Eq. (3) or (4) by using the basis vectors.

In the light of the above discussion, we obtain partial transposes $\rho_{12}^{t_1}$ and $\rho_{13}^{t_1}$ of the reduced density matrices. For example, after tracing out the third spin-half system, the partial transpose $\rho_{12}^{t_1}$ of the reduced density matrix ρ_{12} is written as

$$\rho_{12}^{t_1} = \frac{1}{Z}\begin{pmatrix} a_{11} & a_{12} & 0 & 0 & 0 & 0 \\ a_{21} & a_{22} & 0 & 0 & 0 & 0 \\ 0 & 0 & a_{33} & 0 & 0 & 0 \\ 0 & 0 & 0 & a_{44} & 0 & 0 \\ 0 & 0 & 0 & 0 & a_{55} & a_{56} \\ 0 & 0 & 0 & 0 & a_{65} & a_{66} \end{pmatrix}, \tag{5}$$

where $a_{12} = a_{21}$ and $a_{56} = a_{65}$. Hence the negativity N_{12} for the (1/2, 1) system is given by

$$\begin{aligned} &N(\rho_{12}) \\ &= \frac{1}{2}\max\left[0, \sqrt{(a_{11}-a_{22})^2 + 4a_{21}^2} - a_{11} - a_{22}\right] \\ &\quad + \frac{1}{2}\max\left[0, \sqrt{(a_{55}-a_{66})^2 + 4a_{65}^2} - a_{55} - a_{66}\right]. \end{aligned} \tag{6}$$

After tracing out the second spin-1, the partial transpose $\rho_{13}^{t_1}$ of the reduced density matrix ρ_{13} is written as

$$\rho_{13}^{t_1} = \frac{1}{Z}\begin{pmatrix} a'_{11} & 0 & 0 & a'_{41} \\ 0 & a'_{22} & 0 & 0 \\ 0 & 0 & a'_{33} & 0 \\ a'_{14} & 0 & 0 & a'_{44} \end{pmatrix}, \tag{7}$$

where $a'_{11} = a'_{44}$, $a'_{14} = a'_{41}$, and $a'_{22} = a'_{33}$. Finally, the negativity N_{13} for the (1/2, 1/2) system is given in terms of the matrix elements of Eq. (7) as

$$N(\rho_{13}) = \max\left[0, \left|a'_{41}\right| - a'_{11}\right]. \tag{8}$$

Now we can compute $N(\rho_{12})$ and $N(\rho_{13})$. However, it is very tedious to write out the explicit elements of $\rho_{12}^{t_1}$ and $\rho_{13}^{t_1}$ due to the complexity of matrix ρ. So we will compute numerically and discuss the numerical results of $\rho_{12}^{t_1}$ and $\rho_{13}^{t_1}$ in Eqs. (5) and (7), $N(\rho_{12})$ and $N(\rho_{13})$ in Eqs. (6) and (8), respectively.

3. Numerical results

In this section, we present the numerical results of the thermal entanglement between spins in the three-spin (1/2, 1, 1/2) anisotropic Heisenberg XXZ system under an inhomogeneous magnetic field. The negativities N_{12} and N_{13} for F and AF interactions are presented in the following subsections respectively.

3.1. Thermal entanglement between spins (1/2, 1) in the system

To witness the entanglement between spins (1/2, 1) in the three-spin (1/2, 1, 1/2) anisotropic Heisenberg XXZ system under an inhomogeneous magnetic field for F and AF interactions, the negativity N_{12} in Eq. (6) is obtained after computing numerically the elements of matrix $\rho_{12}^{t_1}$. The obtained results are given below.

The magnetic field dependences of the negativity N_{12} for stagger magnetic fields $b = 0$ and $b = 0.5$ at fixed anisotropy parameter $\gamma = 0.5$ and temperature $T = 0.01$ are shown in Fig. 2(a) for the F case $J = -1$, and in Fig. 2(b) for the AF case $J = 1$. As can be seen from Fig. 2, typically, two plateaus appear in the negativity curve depending on the external magnetic field B when other parameters of the Hamiltonian are fixed.

The transition from the first plateau to the second plateau occurs at a critical magnetic field B_{c1} where the negativity N_{12} has a singularity, and the second entanglement plateau suddenly drops to zero at the second critical magnetic field B_{c2}. The stagger magnetic field does not play any role in the plateau mechanism, however, it changes the width and the height of the entanglement plateau. To explain the entanglement plateau in the negativity curve, we can use an analogy between entanglement and magnetization, since the entanglement is also a qualitative measure of the correlations between spins as the magnetization. Haldane predicted[28,29] that the energy gap between the singlet ground states and the first excited triplet states in spin systems can originate from frustration, dimerization, single-ion anisotropy, or periodic fields and lead to a plateau behavior in magnetization under an external magnetic field. The number of the magnetic plateaus is simply determined by the $2s+1$ condition. In the case of mixed spins, the number of the plateaus is dominated by the higher spin in the system. In our study, we observe three plateaus (two non-zero entangled plateaus and one non-entangled plateau at zero), the number is equal to that of the magnetic plateaus in magnetization.[30,31] Hence the number of plateaus suggests that the entangled plateaus are caused by the energy gap between the singlet ground states and the first excited triplet states in the system. Therefore, the facts allow us to use the analogy of the behaviors between the entanglement and the magnetic plateaus of the spin system.

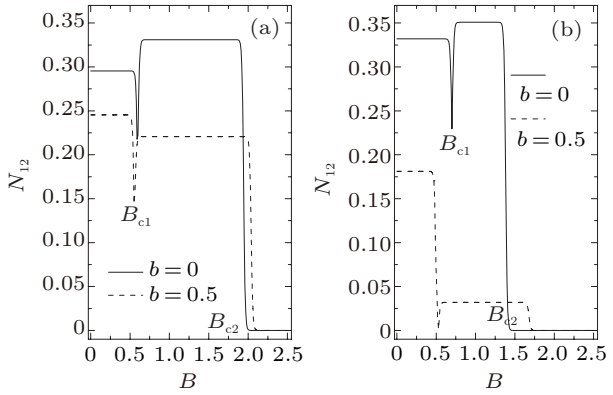


Fig. 2. Magnetic field dependences of N_{12} for arbitrary anisotropy and staggered magnetic fields at very low temperature: (a) F case $J=-1$, (b) AF case $J=1$. The parameters are set as $\gamma=0.5$ and $T=0.01$.

The critical behavior in negativity N_{12} clearly depends on all parameters of Hamiltonian (1). The anisotropy and the temperature play significant roles like the external magnetic field on the entanglement behavior in the system. Therefore, to investigate the anisotropy dependence of the critical behavior of negativity N_{12}, critical B_c is plotted versus the anisotropy in Fig. 3 for F and AF cases at a fixed temperature and staggered field. As can be seen from Figs. 3(a) and 3(b), B_{c1} and B_{c2} linearly increase with increasing anisotropy γ for a fixed temperature and staggered field. The widths of the plateaus also linearly decrease when the anisotropy parameter decreases from one to zero. For $\gamma>0$, the system behaves as the XXZ system, and when $\gamma=0$, the system reduces to the XX system. The plateau at $\gamma=0$ in Fig. 3 is that in the entanglement occurring in the three-spin (1/2, 1, 1/2) XX Heisenberg spin system.

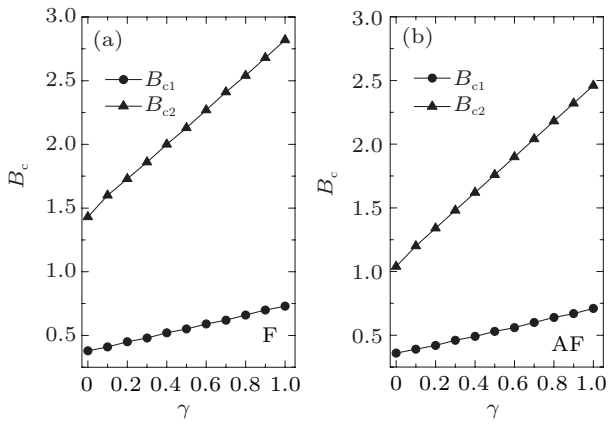


Fig. 3. Anisotropy dependences of N_{12} in the XXZ system with $B=1$, $b=0.5$, and $T=0.01$: (a) F case $J=-1$, (b) AF case $J=1$.

To investigate the temperature dependence of the entanglement between spins, the negativity N_{12} for fixed $J=\pm1$, $\gamma=0.5$, $B=1$, and $b=0.5$ is plotted as a function of the temperature in Fig. 4. It can be seen from the figure that, in the F case ($J=-1$), the negativity N_{12} decreases monotonically with increasing temperature and finally reaches to zero at the critical temperature T_c. The thermal entanglement in the F case is more sensitive to the temperature than that in the AF case, however, the negativity N_{12} in the AF case ($J=1$) exhibits a very interesting behavior. Indeed, the negativity in the AF case firstly decreases with increasing temperature T and reaches to zero at T_{c1}. Then the negativity shows a smooth revival until a maximum value due to the optimal of all eigenstates in the system. After that it collapses gradually to zero at the second critical temperature T_{c2}. The critical behavior at T_{c1} in the negativity N_{12} for the AF case may be a signature of the quantum phase transition at finite temperature. We notice that the quantum phase transition is purely driven by quantum fluctuations where the de Broglie wavelength is greater than the correlation length of the thermal fluctuations[32,33] and is generally expected at absolute zero temperature. In recent studies, the quantum phase transition in the entanglement of two or more qubits has been observed at the absolute zero temperature.[34–38] However, the quantum phase transition can also occur at near absolute temperature when the thermal fluctuations are negligible.[32,39,40] At finite temperature, if the system resists to the thermal fluctuation due to the entanglement between particles, quantum fluctuations may survive in the system and lead to the quantum phase transition (see Ref. [41]). The quantum phase transition in entanglement of two or more qubits has been observed at finite temperature.[32,38–40,42] Therefore, in this study, the critical point T_{c1} may indicate the presence of the quantum phase transition in entanglement for the AF interaction.

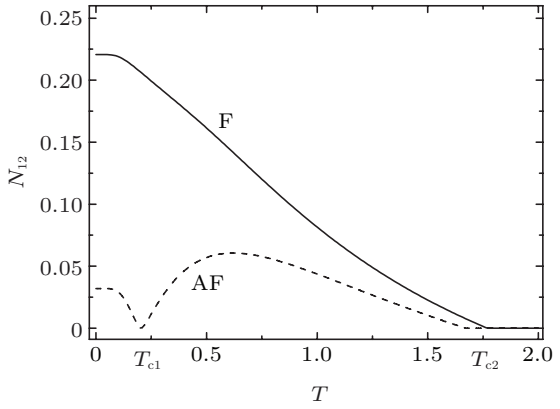


Fig. 4. The N_{12} as a function of temperature T at $B=1$, $b=0.5$, and $\gamma=0.5$ for F ($J=-1$) and AF ($J=1$) cases.

Finally, in order to study the anisotropy γ and magnetic field B dependences of the critical temperature, the T_c–γ and T_c–B phase diagrams for F and AF cases are plotted in Fig. 5. As can be seen in Fig. 5(a), the critical point T_c for the F case linearly changes with the anisotropy. However, unlike the F case, in Fig. 5(b), there are two critical points for the AF case. The critical temperature T_{c1} slightly increases for small anisotropy, then remains almost constant for increasing anisotropy. Whereas the critical temperature T_{c2} smoothly increases with increasing anisotropy, and for large anisotropy,

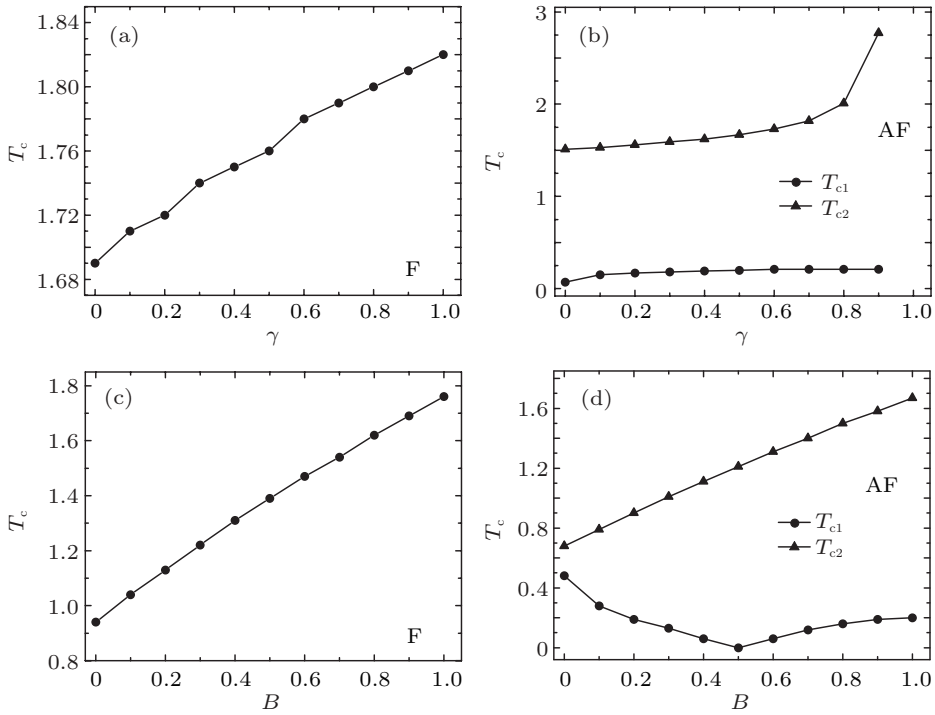


Fig. 5. For fixed $T = 0.01$, $B = 0.5$, and $b = 0.5$, N_{12} as a function of the anisotropy γ: (a) F case, (b) AF case. For fixed $T = 0.01$, $\gamma = 0.5$, and $b = 0.5$, N_{12} as a function of the magnetic field B: (c) F case, (d) AF case.

it increases exponentially with increasing anisotropy. On the other hand, it can be seen in Fig. 5(c) that the critical point T_c for the F case linearly changes with the external magnetic field. For the AF case, in Fig. 5(d), the critical temperature T_{c1} linearly increases with increasing B. However, the critical temperature T_{c2} linearly decreases up to a critical B, and then this critical point linearly increases with increasing magnetic field.

3.2. Thermal entanglement between spins (1/2, 1/2) in the system

To measure the entanglement between spins (1/2, 1/2) in the three-spin (1/2, 1, 1/2) anisotropic Heisenberg XXZ system under an inhomogeneous magnetic field for F and AF interactions, the negativity N_{13} in Eq. (8) is obtained after computing numerically the elements of the matrix $\rho_{13}^{t_1}$. The obtained results are presented below.

The magnetic field dependence of the negativity N_{13} for staggered magnetic fields $b = 0$ and $b = 0.5$ at fixed anisotropy parameter $\gamma = 0.5$ and temperature $T = 0.01$ are shown for F case $J = -1$ and AF case $J = 1$ in Figs. 6(a) and 6(b), respectively. As it can be seen from Fig. 6, typically, two plateaus appear in the negativity curve in the F case, however, only one plateau appears for the AF interaction with two critical points. The transitions between plateaus are quite straight and occur at B_{c1} and B_{c2}. However, there is no singularity at B_{c1} in the N_{13} curve unlike N_{12}. For the F case, the first plateau in Fig. 6(a) appears up to critical point B_{c1}, then the second plateau occurs between B_{c1} and B_{c2} where the entanglement drops to zero. For the AF case, a nonzero plateau only appears between B_{c1} and B_{c2}. Here the stagger magnetic field does not play any role in the plateau mechanism either, however it changes the width and the height of the entanglement plateau.

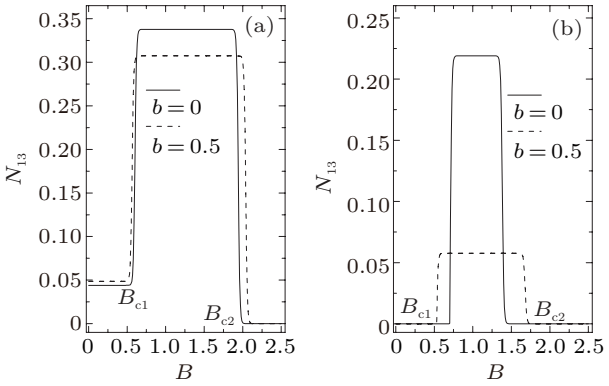


Fig. 6. Magnetic field dependence of N_{13} for arbitrary anisotropy and staggered magnetic field at very low temperature: (a) F case $J = -1$, (b) AF case $J = 1$. The parameters are set as $\gamma = 0.5$ and $T = 0.01$.

In order to study the effect of the anisotropy on the critical point B_c, Fig. 7 is plotted for a fixed temperature and staggered field. As can be seen from Fig. 7, B_{c1} and B_{c2} linearly increase with increasing anisotropy γ for the fixed temperature and staggered field. This behavior indicates that the width of the plateau also linearly decreases when the anisotropy decreases from one to zero. Similarly for $\gamma > 0$, the three-spin (1/2, 1, 1/2) F and AF triangle behaves as the XXZ system, and when $\gamma = 0$, the system reduces to the XX system. Hence we can conclude that the plateau behavior in entanglement between spins (1/2, 1/2) occurs in the three-spin (1/2, 1, 1/2) XX Heisenberg spin system.

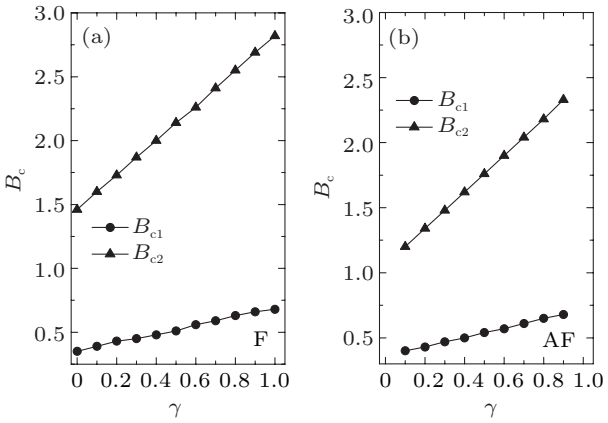


Fig. 7. Anisotropy dependences of N_{13} in the XXZ system with $B = 1$, $b = 0.5$, and $T = 0.01$: (a) F case $J = -1$, (b) AF case $J = 1$.

The temperature dependences of negativity N_{13} for F and AF cases at $J = \pm 1$, $\gamma = 0.5$, $B = 1$, and $b = 0.5$ are shown in Fig. 8. It can be seen from the figure that the thermal entanglement in the F case is more sensitive to the temperature than that in the AF case. The negativity N_{13} decreases monotonically with increasing temperature T and finally reaches to zero at a critical temperature T_c for both F and AF cases. The critical point T_c for the AF case is smaller than that for the F case. On the other hand, no trace of quantum phase transition in the temperature dependence of N_{13} is seen, unlike N_{12}.

Finally, the T_c–γ and T_c–B phase diagrams for F and AF cases are drawn in Fig. 9. These phase diagrams present the anisotropy γ and magnetic field B dependences of the critical temperature. As can be seen in Fig. 9(a), the critical point T_c has a constant value with increasing anisotropy up to critical anisotropy γ_c, after the critical point T_c for the F case, it linearly changes with increasing anisotropy. Unlike the F case, in Fig. 9(b), the critical temperature T_c slightly increases up to critical anisotropy γ_c, passes through a maximum value, then almost linearly decreases with increasing anisotropy. On the other hand, as shown in Fig. 9(c), the critical temperature T_c linearly increases with increasing B in the F case. In the AF case, the critical temperature T_c is zero up to a critical magnetic field B_c, after this critical point, T_c linearly increases with increasing magnetic field B.

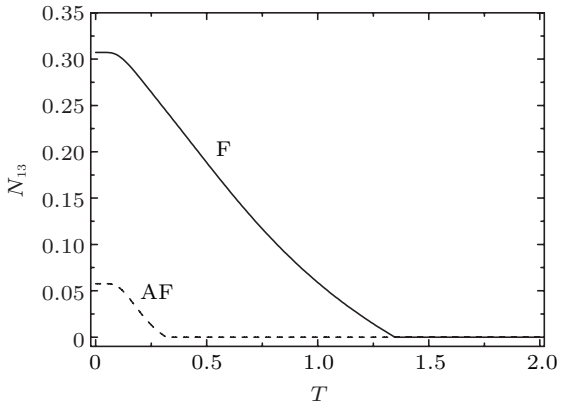


Fig. 8. The N_{13} as a function of temperature T at $B = 1$, $b = 0.5$, and $\gamma = 0.5$ for the F ($J = -1$) and AF ($J = 1$) cases.

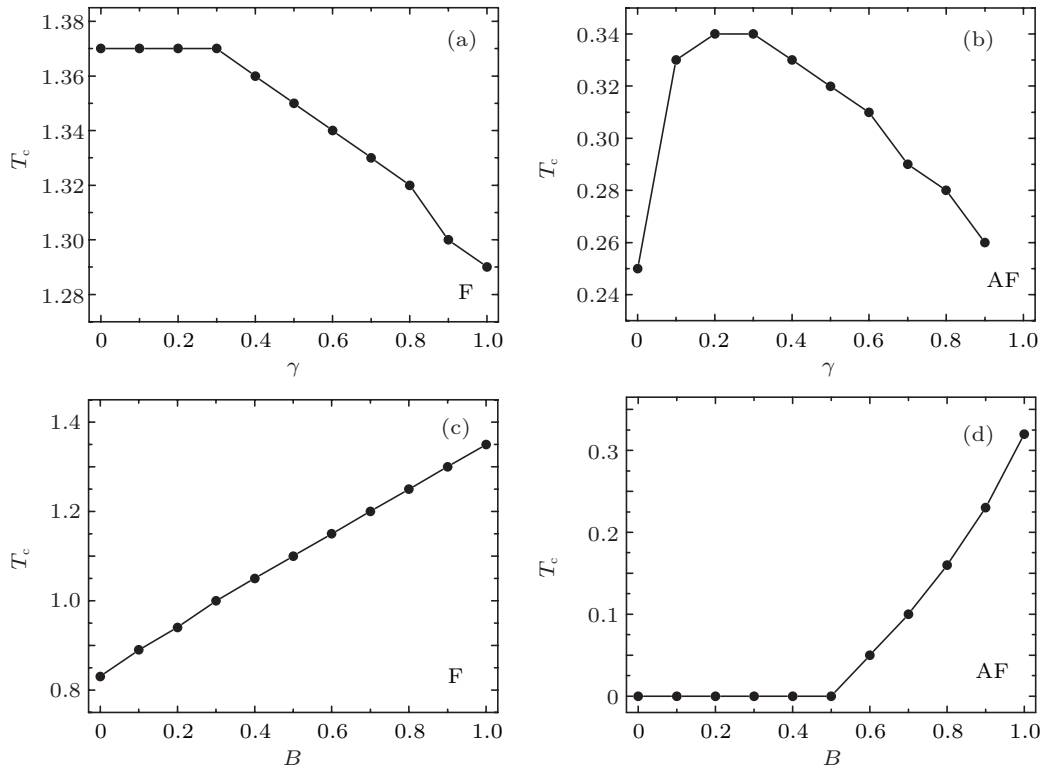


Fig. 9. For fixed $T = 0.01$, $B = 0.5$, and $b = 0.5$, N_{13} as a function of the anisotropy γ in (a) the F case and (b) the AF case. For fixed $T = 0.01$, $\gamma = 0.5$, and $b = 0.5$, N_{13} as a function of the magnetic field B in (c) the F case and (d) the AF case.

4. Conclusion

In this study, considering the three-mixed-spin (1/2, 1, 1/2) anisotropic Heisenberg XXZ system on a simple triangular cell under an inhomogeneous magnetic field at equilibrium, we numerically investigate the thermal pairwise entanglement in terms of the negativity of spins (1/2, 1) and spins (1/2, 1/2) depending on the parameters of Hamiltonian (1). We show that different and strong entanglement plateaus in negativity curves of N_{12} and N_{13}, which correspond to the thermal entanglements of spin pairs (1/2, 1) and (1/2, 1/2), respectively, occur depending on the external magnetic field for fixed parameters of the Hamiltonian for both F and AF interactions. The numerical results reveal that the appearance or disappearance of the entanglement plateaus and the transition between these plateaus occur at different critical magnetic fields. The height and width of the plateau are affected by the anisotropy, the stagger magnetic field, and the interaction type of Hamiltonian (1). We conclude that the plateau behaviors in the thermal entanglement curves are caused by the energy gap between the singlet ground states and the first excited triplet states. On the other hand, we also separately investigate the temperature dependences of N_{12} and N_{13} for both F and AF cases. The negativities N_{12} for the F case and N_{13} for both F and AF cases almost decay exponentially to zero at a critical temperature with increasing temperature. Surprisingly, we observe two critical points T_{c1} and T_{c2} in the entanglement curve of N_{12} for the AF case. The first critical point T_{c1} in the entanglement curve of N_{12} for the AF case may be a signature of the presence of the quantum phase transition at finite temperature in the triangular cell with three mixed XXZ Heisenberg spins.

Acknowledgments

Authors acknowledge Ozgur E. Mustecaplioglu for valuable comments, and one of the authors (SDH) thanks to Tugba Tufekci-Sen for her kind assistance with this work.

References

[1] Nielsen M A and Chuang I A 2000 *Quantum Computing and Quantum Information* (Cambridge: Cambridge University Press)
[2] Schumacher B 1996 *Phys. Rev. A* **54** 2614
[3] Loss D and Divincenzo D P 1998 *Phys. Rev. A* **57** 120
[4] Bukard G, Loss D and Divincenzo D P 1999 *Phys. Rev. B* **59** 2070
[5] Imamoglu A 1999 *Phys. Rev. Lett.* **83** 4204
[6] Platzman P M and Dykman M I 1999 *Science* **284** 1967
[7] Raussendorf R and Briegel H J 2001 *Phys. Rev. Lett.* **86** 5188
[8] Bennett C H 1993 *Phys. Rev. Lett.* **70** 1895
[9] Bennett C H and Wiesner S J 1992 *Phys. Rev. Lett.* **69** 2881
[10] Divincenzo D P 1995 *Science* **270** 255
[11] Bose S 2007 *J. Contemp. Phys.* **48** 13
[12] Kay A 2010 *Int. J. Quantum Inf.* **8** 641
[13] Christandl M, Datta N, Ekert A and Landahl A J 2004 *Phys. Rev. Lett.* **92** 187902
[14] Ekert A K 1991 *Phys. Rev. Lett.* **67** 661
[15] Deutsch D 1996 *Phys. Rev. Lett.* **77** 2818
[16] Shor P W 1997 *SIAM Journal on Computing* **26** 1484
[17] Grover L K 1997 *Phys. Rev. Lett.* **79** 325
[18] Karlsson A and Bourennane M 1998 *Phys. Rev. A* **58** 4394
[19] Gorbachev V N and Trubilko A 2000 *Journal of Experimental and Theoretical Physics* **91** 894
[20] Hao J C, Li C F and Guo G C 2001 *Phys. Rev. A* **63** 054301
[21] Brub D, DiVincenzo D P, Ekert A, Fuchs C A, Macchiavello C and Simolin J A 1998 *Phys. Rev. A* **57** 2368
[22] Sun Z, Wang X, Hu A and Li Y Q 2006 *Physica A* **370** 483-500
[23] Shun W L, Hui J and Xiang-Mu K 2012 *Acta Phys. Sin.* **61** 240304 (in Chinese)
[24] Wootters W K 1998 *Phys. Rev. Lett.* **80** 2245
[25] Peres A 1996 *Phys. Rev. Lett.* **77** 1413
[26] Horodecki M et al 1996 *Phys. Lett. A* **223** 1
[27] Vidal G and Werner R F 2002 *Phys. Rev. A* **65** 032314
[28] Haldane F D M 1983 *Phys. Rev. Lett.* **50** 1153
[29] Haldane F D M 1983 *Phys. Lett. A* **93** 464
[30] Oshikawa M 1997 *Phys. Rev. Lett.* **78** 1984
[31] Aydiner E 2004 *Chin. Phys. Lett.* **21** 2289
[32] Werlang T, Ribeiro G A P and Rigolin G 2013 *Int. J. Mod. Phys. B* **27** 1345032
[33] Wu L A, Sarandy M S and Lidar D A 2004 *Phys. Rev. Lett.* **93** 250404
[34] Hu Z N, Yi K S and Park K S 2007 *J. Phys. A: Math. Theor.* **40** 7283
[35] Wang X, Fu H and Solomon A I 2001 *J. Phys. A: Math. Gen.* **34** 11307
[36] Abliz A, Cai J T, Zhang G F and Jin G S 2009 *J. Phys. B: At. Mol. Opt. Phys.* **42** 215503
[37] Zhang X X, Yin X C, Sun G and Shan C J 2010 *Int. J. Theor. Phys.* **49** 1507-1515
[38] Li Y C and Lin H Q 2011 *Phys. Rev. A* **83** 052323
[39] Werlang T and Rigolin G 2010 *Phys. Rev. A* **81** 044101
[40] Werlang T, Trippe C, Ribeiro G A P and Rigolin G 2010 *Phys. Rev. Lett.* **105** 095702
[41] Cuccoli A, Taiti A, Vaia R and Verrucchi P 2007 *Phys. Rev. B* **76** 064405
[42] Rong C R, Jie X Y and Xiao M Z 2010 *Chin. Phys. B* **19** 050304